AIP | The Journal of Chemical Physics

The high-pressure electronic structure of the [Ni(ptdt)2] organic molecular conductor

P. R. Tulip, S. P. Bates, and S. J. Clark

Citation: The Journal of Chemical Physics **137**, 024701 (2012); doi: 10.1063/1.4731692
View online: http://dx.doi.org/10.1063/1.4731692
View Table of Contents: http://scitation.aip.org/content/aip/journal/jcp/137/2?ver=pdfcov
Published by the AIP Publishing

The high-pressure electronic structure of the [Ni(ptdt)$_2$] organic molecular conductor

P. R. Tulip,[1] S. P. Bates,[2] and S. J. Clark[1]
[1]*Department of Physics, Science Laboratories, University of Durham, South Road, Durham DH1 3LE, United Kingdom*
[2]*School of Physics and Astronomy, University of Edinburgh, Edinburgh EH9 3JZ, United Kingdom*

(Received 5 May 2012; accepted 12 June 2012; published online 9 July 2012)

The electronic structure of the single component molecular crystal [Ni(ptdt)$_2$] (ptdt = propylenedithiotetrathiafulvalenedithiolate) is determined at ambient and high pressure using density functional theory. The electronic structure of this crystal is found to be of the "crossing bands" type with respect to the dispersion of the HOMO and LUMO, resulting in a small, non-zero density of states at the Fermi energy at ambient pressure, indicating that this crystal is a "poor quality" metal, and is consistent with the crystal's resistivity exhibiting a semiconductor-like temperature dependence. The ambient pressure band structure is found to be predominantly one-dimensional, reflecting enhanced intermolecular interactions along the [100] stacking direction. Our calculations indicate that the band structure becomes two-dimensional at high pressures and reveals the role of shortened intermolecular contacts in this phenomenon. The integrity of the molecular structure is found to be maintained up to at least 22 GPa. The electronic structure is found to exhibit a crossing bands nature up to 22 GPa, where enhanced intermolecular interactions increase the Brillouin zone centre HOMO-LUMO gap from 0.05 eV at ambient pressure to 0.15 eV at 22 GPa; this enhanced HOMO-LUMO interaction ensures that enhancement of a metallic state in this crystal cannot be simply achieved through the application of pressure, but rather requires some rearrangement of the molecular packing. Enhanced HOMO-LUMO interactions result in a small density of states at the Fermi energy for the high pressure window 19.8–22 GPa, and our calculations show that there is no change in the nature of the electronic structure at the Fermi energy for these pressures. We correspondingly find no evidence of an electronic semiconducting-metal insulator transition for these pressures, contrary to recent experimental evidence [Cui *et al.*, J. Am. Chem. Soc. **131**, 6358 (2009)]. © *2012 American Institute of Physics*. [http://dx.doi.org/10.1063/1.4731692]

I. INTRODUCTION

Recent decades have witnessed intense research efforts into the physics and chemistry of molecular conductors.[1–3] Any candidate system must satisfy two criteria, viz., that there exist electronic bands formed through intermolecular interactions and second, that there must exist some process of generating charge carriers.[3,4] As a consequence, early research focussed upon two-component molecular materials, in which one, or both, components from electronic bands, and where charge generation is effected through charge transfer from one component to another. Examples include (TMTSF)$_2$PF$_6$,[5,6] in which TMTSF (tetramethyltetraselenafulvalene) molecules constitute a band, and charge transfer is achieved by transfer from TMTSF molecules to the PF$_6$ species, and (TTF)(TCNQ) (TTF = tetrathiafulvalene; TCNQ = tetracyanoquinodimethane).[2,3,7]

One aim of such research has been to develop a single-component organic conductor. This is a challenging task, as molecules usually possess an even number of electrons, and thus all orbitals are doubly occupied. In conjunction with a large HOMO-LUMO gap, it is therefore difficult to envisage, naively, how a single-component molecular conductor can be formed. While it could be naively suggested that one should utilise a molecule with a half-filled HOMO, such that a half-filled band is obtained, such a structure is (if quasi-one-dimensional) liable to undergo a Peierls transition,[8] resulting in an insulating ground state; if it is not quasi-one-dimensional, then the on-site Coulomb repulsion is such as to localise the unpaired electron on each molecular site, resulting in a Hubbard insulator.[3]

Band structure engineering has provided a more fruitful approach; this involves a careful choice of molecular entity such that the crystal possesses a nonvanishing Fermi surface and is hence metallic. A recent review[3] has discussed in depth the criteria that must be satisfied if a metallic state is to result; however, in the interests of ensuring the clarity of our subsequent discussions, we shall briefly paraphrase and summarise these results here. In the absence of charge generation by charge transfer from a donor to an acceptor moiety, a crystal must be designed such that internal charge transfer may occur. This may be achieved by HOMO-LUMO electron transfer, which in turn demands that both the HOMO and LUMO bands cross the Fermi energy; the resulting *two band* system will thus possess a partially occupied LUMO and HOMO, with the consequence that both electron and holes will be able to act as charge carriers within the crystal.

Although conceptually elegant and appealing, achieving this state is more challenging: internal charge transfer will

only occur if both the LUMO and HOMO bands cross the Fermi level, which requires that the HOMO-LUMO gap be smaller than the bandwidth. This may be stated mathematically as $(W_{LUMO} + W_{HOMO})/2 > \Delta$, where W refers to the width of the requisite band, and Δ is the HOMO-LUMO gap. Achieving the metallic state thus necessitates that a molecule with a small gap be chosen; secondly, that a crystal structure must be engineered in which significant intermolecular interactions occur (so-called overlap modes) such that a large bandwidth is achieved.

Both of these criteria may be satisfied by employing extended-TTF dithiolate ligands, in which π-electron ligands bond to a metallic atom. *Ab initio* calculations indicate that such systems possess small HOMO-LUMO gaps,[9] which may be achieved as follows: the HOMO and LUMO are constructed from in-phase and out-of-phase combinations, respectively, of the ligand π-orbitals. The LUMO, in contrast to the HOMO, may, by symmetry, mix with the metal ion *d*-orbitals, although the degree of mixing is weak. This results in a weak metal-ligand interaction, and a small HOMO-LUMO splitting. Altering the size of the organic ligand modifies the degree of π-d mixing, and thus the size of the HOMO-LUMO gap, with larger ligands leading to smaller gaps. The use of π-electron systems achieves significant intermolecular overlap, leading to the desired combination of small HOMO-LUMO splitting and large bandwidth.

The above criteria are necessary, but not sufficient, to obtain a single-component molecular metal. To understand why this is the case, one must consider the nature of the intermolecular overlap modes. If one characterises the overlap modes through overlap integrals t, then if the HOMO-HOMO and LUMO-LUMO interactions possess overlap integrals of opposite sign, this will result in an intended crossing of the HOMO and LUMO bands (so-called "crossing bands"); the resulting HOMO-LUMO interaction will then yield a HOMO-LUMO splitting, opening up a bandgap and destroying the metallic state. There are two possible remedies: engineering a crystal structure such that HOMO-HOMO and LUMO-LUMO overlap integrals are of the same sign, yielding so-called parallel bands, or ensuring that a three-dimensional network of intermolecular contacts forms. These may lead to finite bandwidth, and thus stabilisation of the metallic state, even in cases in which the HOMO and LUMO interact.

Recent work[10] has also raised the possibility of the achieving a metallic state through the application of pressure to a single-component semiconducting molecular crystal. While the pressure-induced metallisation of inorganic semiconductors such as germanium and silicon is well-known, in molecular crystals the metallicity condition implies that the bandwidth (dictated by relatively weak intermolecular interactions) is enhanced by pressure such that it is comparable to the HOMO-LUMO gap (dictated by strong intramolecular interactions); this suggests that it will be difficult to achieve the metallic state while preserving the integrity of the molecular structure. Indeed, such a breakdown in molecular structure is observed in the pressure-induced metallisation of the I_2 molecular crystal.[10–12]

Contrary to this, Cui *et al.*[13] and Kobayashi *et al.*[14] recently studied pressure-induced metallisation in [Ni(ptdt)$_2$)] (ptdt = propylenedithiotetrathiafulvalenedithiolate) and provided evidence that it is indeed possible to metallise organic molecular crystals through the application of pressure while preserving the molecular structure. These authors demonstrated, through electrical resistivity measurements, that this crystal exhibits a narrow window of metallic behaviour between approximately 19 and 20.7 GPa, and that without this range, it exhibits semiconducting behaviour.

The [Ni(ptdt)$_2$] system is of interest as it served as a prototypical system that was used by Kobayashi *et al.*[15] to derive the set of "design rules" that we outline above. *Ab initio* calculations of the singlet and lowest lying triplet energies of isolated molecules of [Ni(ptdt)$_2$] indicate that this molecule possesses a very small HOMO-LUMO gap.[15] Tight-binding Hückel calculations suggest that the crystal possesses a quasi-one-dimensional electronic band structure of a crossing-band type.[15] At ambient pressure, a Fermi surface exhibiting small electron and hole pockets is stabilised by transverse intermolecular interactions. This, in conjunction with the temperature-dependent resistivity of the crystal, has been taken as evidence that it is a narrow-band semiconductor,[13–16] whilst the stability of this semiconducting structure up to approximately 19 GPa indicates that the crystal possesses a crossing-band electronic structure up to high pressures.[13]

To understand the remarkable stability of the semiconducting state in this crystal, and possible structural changes that may result in the stabilisation of a metallic state at high pressure, demands a detailed knowledge of the crystal's electronic structure. Recent work by the current authors[17] concerning the high-pressure electronic structure of the TMTTeN molecular crystal and by Rovira *et al.*[9] examining the electronic structure of the Ni(tmdt)$_2$ molecular metal indicates that simple calculations of the Hückel type can provide a description that is at odds with that provided by state-of-the-art *ab initio* methods such as density functional theory. Questions may also be raised concerning the transferability of the Hückel method; if overlap integrals are parametrised at ambient pressure, it is not immediately obvious that such integrals are applicable in high pressure environments, in particular if the high pressure structure sees distinct changes in the molecular and/or electronic structure. A particular advantage of the first principles approach is that it is a relatively straightforward matter to determine the equilibrium molecular geometry and crystal structure associated with any particular pressure, in contrast to the Hückel method, in which one must make an intelligent guess as to what the high pressure crystal structure and the molecular HOMO-LUMO gap will be.

Recent first principles calculations and experiments by Zhou *et al.*[18] on the closely related [Au(ptdt)$_2$] molecular conductor reveal that it possesses a flattened cylindrical two-dimensional Fermi surface, with a room temperature conductivity of 2 S cm^{-1} for a compressed pellet sample (compared to 7 S cm^{-1} for single crystal [Ni(ptdt)$_2$] (Ref. 13)), and a temperature-dependence resistivity that is similar to that of the [Ni(ptdt)$_2$] crystal. Despite this, it has been characterised as being "essentially metallic," in contradistinction

to the "semiconducting" character of $[Ni(ptdt)_2]$. It is timely therefore, given the absence of *ab initio* data concerning this crystal, to apply state-of-the-art *ab initio* electronic structure calculations to examine and understand pressure-induced changes in the electronic structure. To that end, in this work we apply Hohenberg-Kohn-Sham density functional theory (DFT).[19,20] The paper is structured as follows: in Sec. II we describe the computational approach employed in this work; in Sec. III, we present and discuss details of the crystal and electronic structure at ambient and high pressures, and in Sec. IV we present our conclusions.

II. COMPUTATIONAL APPROACH

We perform our calculations within the plane-wave pseudopotential framework as implemented within the CASTEP code.[21] Electron-ion interactions are treated using Vanderbilt ultrasoft pseudopotentials,[22] while the valence electron wavefunctions are expanded in a plane wave basis set with a kinetic energy cutoff of 500 eV, which converges total energies to better than 1 meV/atom; Brillouin zone integrations are performed using a $2 \times 2 \times 2$ Monkhorst-Pack grid.[23] This yields two symmetry-reduced symmetry k-points and converges total energies to the same degree as the kinetic energy cutoff. Exchange and correlation (XC) effects are treated using the generalised gradient approximation (GGA) of Perdew and Wang,[24] which is known to be capable of accurately treating electronic interactions in molecular crystals.[25,26]

We take experimentally determined crystal structures, as reported by Kobayashi *et al.*[15] as our initial structures. The equilibrium geometry is determined by minimising the forces acting on nuclei using a BFGS algorithm, which allows the unit cell to relax, in addition to the atomic degrees of freedom. The convergence criteria are as follows: atomic forces are converged to within 1×10^{-2} eV/Å; stresses are converged to within 1×10^{-1} GPa, and energies are converged to within 1×10^{-6} eV/ion.

Upon successful determination of the equilibrium crystal structure, the Kohn-Sham equations are solved at a series of reciprocal space points to determine the Kohn-Sham band structure. It should be pointed out that semi-local functionals such as the GGA suffer from the well-known "bandgap problem,"[27] viz., a tendency to underestimate the magnitude of bandgaps. To investigate possible sensitivity with respect to XC functional, we determine, at ambient pressure, the band structure at the PW91-derived geometry using the screened exchange (sX) hybrid functional.[28] This mixes Thomas-Fermi screened Hartree-Fock exchange with the LDA, and provides an improved determination of bandgaps in a range of solids.[28] We have also performed spin-polarised calculations to investigate whether the $[Ni(ptdt)_2]$ crystal exhibits any magnetic behaviour. We note here that we have been unable to obtain a magnetic ground state.

This procedure is carried out at the following distinct pressures: ambient; 8 GPa; 19.8 GPa; 20.7 GPa; and 22 GPa. The choice of these pressures is motivated as follows: the ambient calculation allows us to understand the key features of the electronic structure, and to make contact with existing tight-binding Hückel calculations in the literature. The high pressure calculations are motivated by the observations of Kobayashi *et al.*[15] that the $[Ni(ptdt)_2]$ crystal retains its semiconducting character to pressures of at least 7 GPa, and Cui *et al.*'s[13] observations that there is a narrow pressure window in which a metallic state is stabilised.

III. RESULTS AND DISCUSSION

A. Crystal and molecular structure

In Figure 1, the structure of an isolated $[Ni(ptdt)_2]$ molecule is shown along with the numbering convention employed in this study, while in Fig. 2, the ambient crystal structure is shown. We note here that, for ease of comparison, our numbering convention is the same as that of Kobayashi *et al.*[15] $[Ni(ptdt)_2]$ crystallises in a monoclinic structure, with space group $C_{2/m}$ and two molecules per unit cell, with the molecules forming a regular column along the a direction, which we show in Figure 2.

In Table I, we present the experimental lattice parameters at ambient pressure and 296 K obtained by Kobayashi *et al.*, and the DFT-optimised high-pressure lattice parameters. Note that for the ambient pressure calculations, in contradistinction to the high pressure cases, we only relax the atomic coordinates and *do not* relax the unit cell itself. This is because, in the $[Ni(ptdt)_2]$ crystal, the intermolecular interactions responsible for crystal stabilisation are principally due to S–S and C–C contacts; these will likely be van der Waals in character. It is well-known that semi-local XC functionals such as the GGA do not describe van der Waals interactions,[27] which manifests itself as a tendency to underbind such crystals resulting in theoretically derived lattice constants that are greater than those obtained experimentally.[25] At high pressure the neglect of van der Waals interactions in the GGA XC functional is not serious, and we may safely relax the unit cell; this may be understood as follows: when we apply pressure to a molecular system, the compressive effect of this is much greater than the weak van der Waals

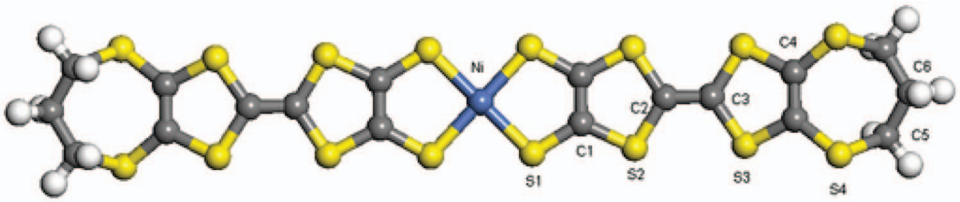

FIG. 1. The molecular structure of the $[Ni(ptdt)_2]$ molecule, illustrating the numbering convention used in this work. Blue indicates Ni; grey C; yellow S; and white H atoms.

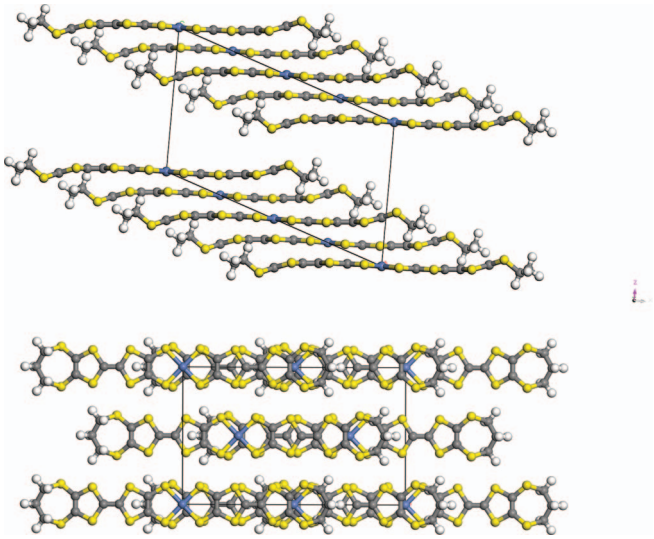

FIG. 2. The crystal structure of the [Ni(ptdt)$_2$] molecular conductor. The upper image shows how molecules stack along the [100] direction, while the lower image shows the transverse overlaps that occur along the [010] direction. The colour code used is as in Fig. 1.

interaction; second, the dominant interactions will become repulsive exchange interactions resulting from wavefunction overlap, which are adequately described by the GGA.

Before considering the optimised molecular geometry, it is worth examining the intermolecular contacts in light of the above discussion. The experimental structure at room temperature possesses short transverse contacts of length 3.526 and 3.618 Å, whereas for our optimised structure we find contacts at 3.576 and 3.693 Å; similarly, experimentally, the shortest S···S contacts are found to occur at 3.446 Å along the stacking direction; our calculations find this distance to be 3.487 Å. The [Ni(ptdt)$_2$] molecules stack so as to maximise both S···S and π-stacking interactions, with the latter being characterised by the C1-C3 and C1-C2 contacts. The Ni atoms are fixed by symmetry on the 2/*m* position, and thus we find that the shortest Ni-Ni contact occurs for both experiment and theory at 7.766 Å. In Table II, we present the non-bonded contacts characterising intermolecular overlap modes as determined from our DFT calculations and compare these with the experimental values. Consistent with the above discussion, our theoretical calculations predict intermolecular contacts that are greater than those found experimentally. Nevertheless, in all cases the level of agreement is within a couple of percent, although it is likely that this is because the unit cell has been fixed at the experimental values.

We now consider the molecular structure itself. In Table III, we present a comparison of intramolecular bond lengths as determined experimentally and from the DFT calculations. The level of agreement observed is similar to that found for the intermolecular contacts, although contrary to the trend observed for intermolecular contacts, in all cases the theoretically derived values are less than the experimental values. Of course, our DFT calculations correspond to the case of absolute zero; it could perhaps be anticipated therefore that part of this discrepancy will owe its origin to the effects of thermal expansion that are neglected in our calculations. We note, however, that comparison with 90 K structural data[15] of Kobayashi *et al.* does *not* suggest that a uniform contraction of the molecular geometry occurs upon cooling. It would seem therefore that the tendency to overbind the molecular geometry relative to experiment is related to the neglect of van der Waals interactions in the GGA XC functional. Our results demonstrate that the PW91 GGA XC functional is capable of providing a sufficiently accurate description of the molecular structure, in agreement with a number of studies.[25,26,29]

We turn now to discuss the effect of pressure upon the crystal and molecular structure. Examining the high pressure lattice parameters in Table I, it is apparent that the largest compression observed is along the *c*-axis, which experiences an approximate 22% reduction in magnitude, compared to

TABLE I. Lattice parameters, unit cell volume and angle β of [Ni(ptdt)$_2$]: experimentally derived values (Kobayashi *et al.*[15]) at ambient pressure and theoretically derived values at high pressure. Experimental values are those obtained at 296 K; all lattice parameters are quoted in Angstroms, volumes in Angstroms,^{3} and angles in degrees.

	Expt.	8 GPa	19.8 GPa	20.7 GPa	22 GPa
a	10.096	9.569	9.299	9.285	9.264
b	11.802	10.694	10.143	10.112	10.072
c	12.420	10.690	9.796	9.752	9.692
Volume	1401.43	1064.06	909.16	901.43	890.91
β	108.74	103.42	100.26	100.10	99.89

TABLE II. Intermolecular contacts: experimental values at ambient pressure and 296 K (Kobayashi *et al.*[15]) and theoretically derived values. All values are quoted in Angstroms.

	Expt.	Ambient	8 GPa	19.8 GPa	20.7 GPa	22 GPa
S1-S2	3.526	3.576	3.143	2.926	2.914	2.898
S1-S1	3.618	3.693	3.150	2.925	2.914	2.898
C1-C3	3.616	3.690	3.291	3.029	3.016	2.995
S1-S3	3.594	3.634	3.154	2.932	2.921	2.904
S2-S2	3.446	3.487	3.196	2.980	2.969	2.954
S3-C5	3.617	3.676	3.105	2.852	2.840	2.822
C1-C2	3.687	3.755	3.334	3.087	3.076	3.060
Ni-Ni	7.766	7.766	7.175	6.880	6.864	6.842

TABLE III. Experimental[15] and theoretical bond lengths; the former are data for 296 K. All values are quoted in Angstroms.

	Expt.	Ambient	8 GPa	19.8 GPa	20.7 GPa	22 GPa
Ni-S1	2.183	2.152	2.123	2.094	2.093	2.090
S2-C1	1.736	1.721	1.708	1.692	1.691	1.689
S3-C3	1.752	1.726	1.702	1.677	1.676	1.674
S4-C4	1.743	1.722	1.708	1.691	1.689	1.688
C1-C1	1.384	1.373	1.365	1.353	1.353	1.351
C4-C4	1.384	1.350	1.349	1.345	1.345	1.344
S1-C1	1.726	1.697	1.687	1.672	1.671	1.669
S2-C2	1.743	1.726	1.713	1.697	1.696	1.695
S3-C4	1.765	1.730	1.715	1.703	1.702	1.701
S4-C5	1.811	1.801	1.769	1.736	1.734	1.732
C2-C3	1.380	1.363	1.364	1.361	1.361	1.361
C5-C6	1.535	1.506	1.483	1.461	1.460	1.458

approximately 8% and 15% for the *a* and *b* axes, respectively. This compression results in the *b*-axis being the longest unit cell axis for pressures greater than 8 GPa. We have performed high pressure calculations *without* the imposition of symmetry constraints, the results of which indicate that there is no change in the unit cell symmetry under compression. It should be noted that Kobayashi *et al.*[15] only provide structural data at ambient pressure (albeit at two distinct temperatures); consequently, there are no experimental data with which to compare our high-pressure structures. However, there are numerous studies[30–32] that demonstrate the ability of DFT to accurately predict high-pressure structures, and we are correspondingly confident in the optimised structures.

It is tempting to expect that the observed axial compression trends are reflected in the behaviour of the intermolecular contacts under pressure, i.e., that contacts parallel to the *c*-axis shorten more than transverse contacts aligned with the *b*-axis, or contacts along the *a*-axis. However, if we examine the intermolecular contacts in Table II, we find that for the contacts aligned along the stacking (i.e., *c*) axis, that the S2-S2 contacts experience a contraction of approximately 15% from 3.446 Å to 2.954 Å, while for the C1-C2,3 contacts we find a contraction of approximately 19%. This compares to a 19% reduction in the transverse S1-S2 contacts, and a 22% reduction in the transverse S1-S1 interaction. Instead, the reason that we observe increased compression along the *c*-axis as compared to the *b*-axis is simply that the [Ni(ptdt)$_2$] molecule is planar, with the molecular plane parallel to the [010] direction and its normal aligned along the [001] direction. It is therefore not possible to compress along the [010] direction to the same extent as along the [001] direction, as to do so would necessitate a breakdown in the molecular structure of the [Ni(ptdt)$_2$] molecule. This reasoning does not, however, explain why the least compression is found in the *a*-axis. Understanding this requires a more detailed examination of the electronic structure, and we thus postpone discussion of this to a more suitable juncture.

The recent works of Kobayashi *et al.*[14] and Cui *et al.*[13] on the [Ni(ptdt)$_2$] crystal suggests the existence of a window of metallic behaviour between 19 GPa and 20.7 GPa. It is therefore of interest to examine the intermolecular contacts in light of this result, as it could perhaps be anticipated that the change in electronic behaviour is caused by some alteration in the intermolecular contacts. Examination of the data in Table II shows that over the pressure range of 19.8–22 GPa, all of the intermolecular contacts shorten by approximately the same proportion. There does not appear to be anything "special" occurring with respect to the structure as we compress across this pressure range, and it is therefore difficult to see how such structural changes could be invoked to explain a metal-semiconductor transition. This is a point that we return to later when discussing our electronic structure results.

The behaviour of the intramolecular bond lengths upon compression is given in Table III. Our calculations indicate that the [Ni(ptdt)$_2$] molecule's structure is preserved under compression and is furthermore, remarkably resilient and "stiff." Bond lengths in the terminal propylenic groups are "softest" and undergo the greatest contraction. It is noteworthy that there is very little change in the molecular structure over the pressure range of 19.8 GPa–20.7 GPa, and as with the intermolecular contacts, it is likewise difficult to understand any proposed changes in the electronic properties of this crystal in terms of structural changes.

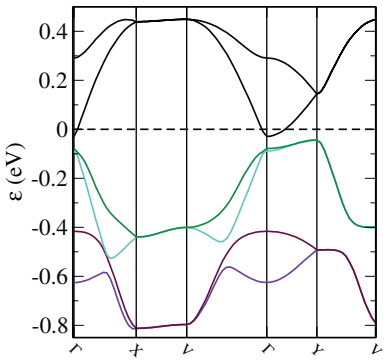

FIG. 3. Electronic band structure of [Ni(ptdt)$_2$] at ambient pressure. The zero of energy (for all band structure plots in this work) has been chosen to be the Fermi energy, which is denoted by a dashed line.

B. Electronic structure

In Figure 3 we present the electronic band structure obtained at ambient pressure. For the purposes of comparison with existing tight-binding calculations of the band structure of this crystal,[15] we consider the same two-dimensional path in reciprocal space. There are certain features which are immediately apparent: first, that the most pronounced dispersion occurs along the [100] direction in the Brillouin zone, and the band structure is therefore predominantly one-dimensional. This direction is aligned approximately along the *a*-axis in the (real space) unit cell, and thus corresponds to the direction in which the largest degree of intermolecular overlap occurs. This is in agreement with tight-binding calculations.[15] Second, the band structure is of the "crossing bands" type, which can be explained with reference to the HOMO-HOMO and LUMO-LUMO overlap integrals.[15] This results in a pronounced HOMO-LUMO interaction at the Γ and Y-points in the Brillouin zone, and thus the opening up of a bandgap. States at these points can be expected to comprise a HOMO-LUMO admixture. It is apparent that despite the opening up of a gap due to this interaction, that the LUMO band cuts the Fermi energy, thus indicating that this crystal has a metallic character.

To investigate the sensitivity of the electronic structure, and in particular, the metallic nature of the crystal to XC functional, we have performed band structure calculations along the line Γ → Y using the sX-LDA functional.[28] We choose this line as it is where the HOMO and LUMO bands exhibit maxima and minima, respectively. Our calculations indicate that the HOMO-LUMO gap at the Γ-point increases from approximately 0.05 eV to approximately 0.15 eV, which is insufficient to alter our conclusions, i.e., the crystal is a poor quality metal.

It is worth noting here that our band structure displays marked differences to existing tight-binding results:[15] we find that the avoided crossings occur at the Γ and Y-points,

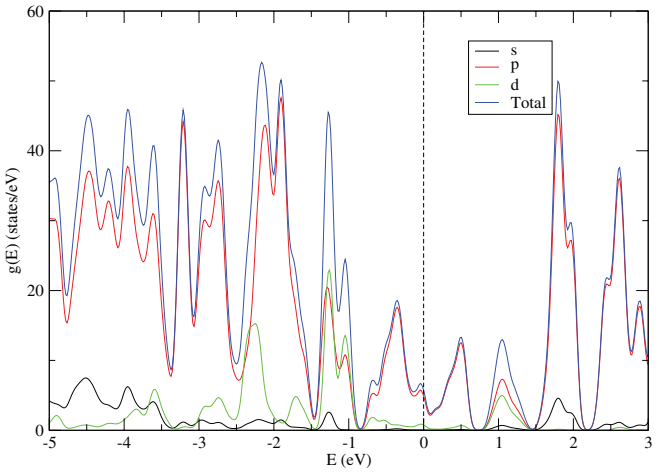

FIG. 4. Partial density of states (PDOS) of $[Ni(ptdt)_2]$ as determined at ambient pressure. The zero of energy (for all pdos plots in this work) has been chosen to be the Fermi energy, which is denoted by a dashed line.

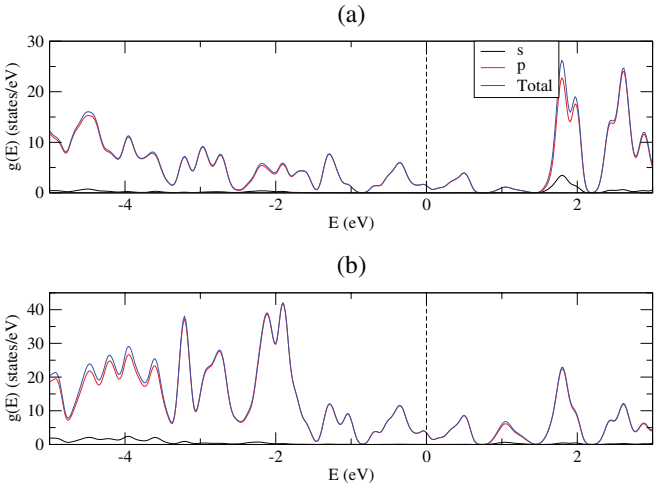

FIG. 5. Partial density of states (PDOS) of $[Ni(ptdt)_2]$ as determined at ambient pressure. In (a) the contribution from carbon atoms is shown, while in (b) we illustrate the contribution from sulphur atoms.

whereas the tight-binding data of Kobayashi *et al.* have these avoided crossings between the V and Γ points, and between the Y and V-points.[15] We find the band structure to be much simpler between Γ and V than is found in the tight-binding calculations. Our calculations display more dispersion in the $\Gamma \rightarrow Y$ direction, indicating that our band structure is less one-dimensional than tight-binding calculations and suggesting that these underestimate the effect of transverse interactions that serve so as to stabilise the metallic state. Similarly, our *ab initio* results display markedly different trends in Davydov splitting across the Brillouin zone, suggesting that the nature of the intermolecular interactions is more pronounced than is allowed for in the simple tight-binding parametrisation of the intermolecular overlaps. We note that similar discrepancies between the results of *ab initio* and tight-binding calculations have been found in the cases of TMTTeN (Ref. 17) and $Ni(tmdt)_2$,[9] where it was concluded (consistent with our results) that tight-binding calculations struggle to capture the balance between the HOMO-LUMO gap and the different intermolecular interactions present.

We mention in passing here that we have determined the band structure for the experimentally determined structure used for the tight-binding calculations (data not shown) and obtain a result that is extremely similar to that in Figure 3, thus demonstrating that the differences between the tight-binding and *ab initio* band structures arise from differences in the treatment of the intermolecular interactions, and not through the use of different geometries.

We may further understand the electronic band structure through the determination of the density of states (DOS) and its decomposition in terms of angular momentum states. In Figure 4 we present the resulting partial density of states (PDOS). It can immediately be seen that, consistent with the band structure, there is a small, yet finite density of states at the Fermi energy, indicating that this crystal is metallic and will have a small Fermi surface at ambient pressure. This is consistent with the tight-binding-derived understanding of the crystal, and consistent with the large room temperature conductivity of approximately 7 S cm^{-1},[13] albeit it is likely that our *ab initio* calculations would predict a different form for the Fermi surface.

This crystal has been characterised in the literature, based upon the temperature dependence of its resistivity, as a narrow-gap semiconductor.[13–15] However, the closely related $[Au(ptdt)_2]$ crystal has recently been characterised as metallic based upon DFT calculations,[18] despite having a lower room temperature conductivity than $[Ni(ptdt)_2]$ (2 S cm^{-1} as opposed to 7 S cm^{-1} in the latter) and displaying a similar temperature dependence to its resistivity; it may therefore be more appropriate and consistent to describe $[Ni(ptdt)_2]$ as metallic, which indicates, contrary to the conclusions of Zhou *et al.*'s,[18] that $[Au(ptdt)_2]$ is not the first, or only, 2D single component layered material to exhibit metallic behaviour.

While it should be emphasised here that our DFT calculations do not incorporate the effect of temperature, and we do not actually determine a theoretical value of the resistivity, it could perhaps be inferred that the form of the DOS explains these observations: at room temperature, the absence of a bandgap will readily allow electrons to occupy conduction band states and contribute to electronic transport, but at low temperature, the number of states available to electrons at the Fermi level that allows them to participate in electronic transport will tend towards the value shown in the PDOS plot, resulting in an increase in the resistivity.

The states in the immediate vicinity of the Fermi energy are found to be primarily of *p*-type character arising from S and C atoms (see Figures 5(a) and 5(b)), with the states above the Fermi energy tending to have more S *p* character than C *p* character. It is of interest to consider this in light of the molecular electronic structure. It is known that the HOMO for this molecule has b_{2g} symmetry and comprises a bonding combination of the two TTF ligand wavefunctions. The HOMO does not possess any Ni *d*-state character, as such mixing is not symmetry-permitted.[15] In contrast, the LUMO, which consists of the antibonding combination of the ligand wavefunctions can indeed mix with the Ni *d*-states.[15,16,33] Consistent with this discussion, we observe that there is no

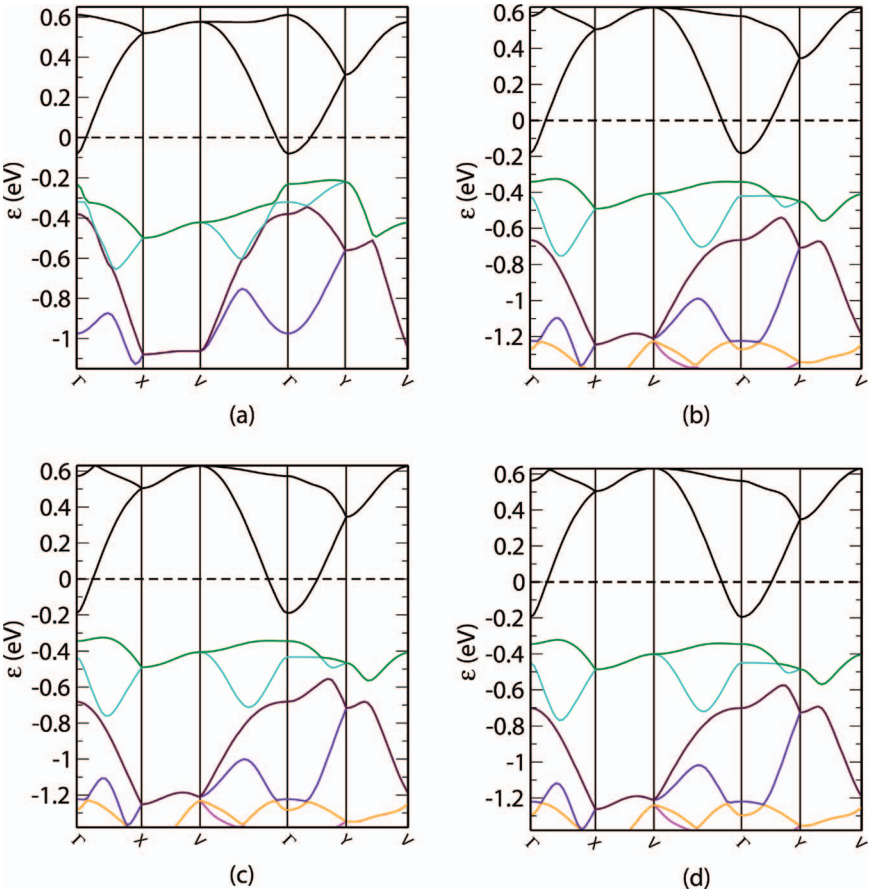

FIG. 6. The evolution of the electronic band structure of [Ni(ptdt)$_2$] under pressure. In (a) we present the result for 8 GPa, (b) 19.8 GPa, (c) 20.7 GPa, and in (d) 22 GPa.

Ni *d* character to the states lying immediately below the Fermi energy; likewise, there is no Ni *d* character to the states immediately above the Fermi energy. This may seem contrary to expectations, based upon the discussion of the molecular electronic structure, but is consistent with the forbidden crossings observed in the band structure, from which it was inferred that these states will be a HOMO-LUMO admixture. As the Ni *d*-states cannot mix with the HOMO states, one should not expect to therefore find any Ni *d*-character in the vicinity of the Fermi energy, and indeed, one instead finds the presence of Ni *d*-states in a well-defined doublet below the Fermi energy and in a single peak at about 1 eV above the Fermi energy. The well-defined nature of these features indicates that the Ni *d*-states are localised.

In Figure 6 we consider the evolution of the electronic band structure under hydrostatic pressure for the pressures 8 GPa, 19.8 GPa, 20.7 GPa, and 22 GPa. If one initially considers the 8 GPa case, then it is apparent that the crossing band nature of the band structure is preserved, while increased dispersion in the $\Gamma \rightarrow$ Y direction is indicative of increased intermolecular interactions, and a more two-dimensional band structure than is observed at ambient pressure. Similarly, the magnitude of the Davydov splitting is increased: e.g., at the Γ-point, the LUMO splitting is increased from 0.32 eV to 0.68 eV. Consistent with this increase in the magnitude of intermolecular interactions, the HOMO-LUMO gap at the Γ-point increases from 0.05 eV at ambient pressure to 0.14 eV at 8 GPa. Examining the PDOS presented in Figure 7, we find that the large density of states from around -5 eV to -1 eV displays more evidence of smearing, consistent with the increased dispersion seen in the band structure. The most significant point, however, is that the crossing-band nature of the band structure ensures that there is still only a small density

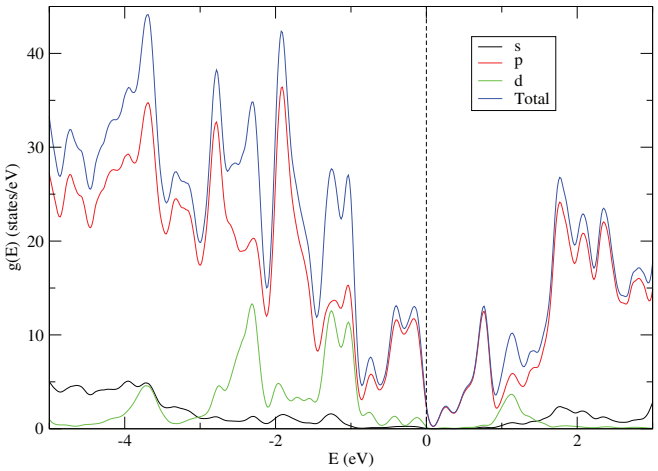

FIG. 7. Partial density of states (PDOS) of [Ni(ptdt)$_2$] as determined at 8 GPa.

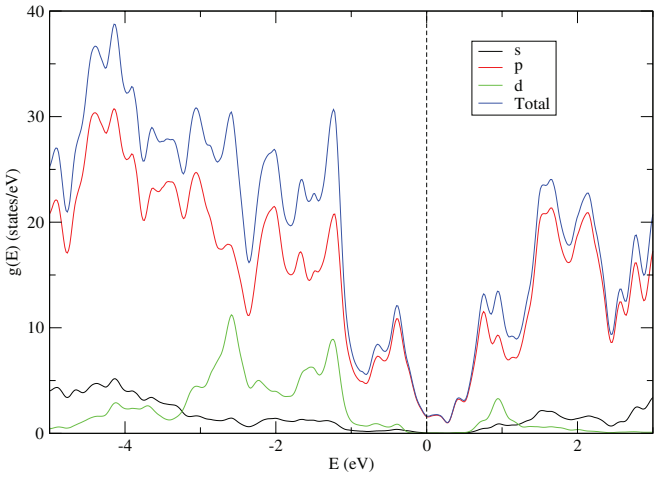

FIG. 8. Partial density of states (PDOS) of $[Ni(ptdt)_2]$ as determined at 22 GPa.

of states at the Fermi energy. This is consistent with measurements that indicate a semiconductor-like temperature dependence to the resistivity at this pressure.[13,14]

This result illustrates an important point, viz.: if one has a crystal with crossing bands, then naively increasing the intermolecular interactions through the application of pressure *will not* stabilise or enhance a metallic state, as the HOMO-LUMO interaction will *also* be increased, and thus the HOMO-LUMO gap will be increased. Instead, stabilisation/enhancement of the metallic state requires that the application of pressure either changes the molecular packing such that the HOMO and LUMO no longer cross, and/or maximises transverse interactions that may stabilise/enhance the metallic state.

We note here that, having examined and understood the nature of the electronic structure of this crystal, we may now understand as to why the least amount of unit cell compression occurs along the [100] direction. As noted above, the band structure plots indicate that the largest degree of intermolecular overlap occurs along the *a*-axis; it is this electronic overlap that will result in the $[Ni(ptdt)_2]$ crystal being resistant to compression along the [100] direction.

It is immediately obvious that the high pressure band structures in Figures 6(b)–6(d) are almost identical. However, the magnitudes of the HOMO-LUMO gap remain almost unaltered for each higher pressure system. This preservation of the HOMO-LUMO gap explains why, examining the PDOS for the 22 GPa case presented in Figure 8 (we do not consider the 19.8 GPa or 20.7 GPa cases further, as they have very similar densities of states), we still find only a small non-zero density of states at the Fermi energy. This result is interesting, as it suggests that the crystal's Fermi surface will be unchanged across the 19.8–22 GPa window, and that it will thus maintain a semiconductor-like temperature dependence to its resistivity. This indicates that it is difficult to enhance a metallic state in this crystal, in agreement with Kobayashi *et al.*[14] and Cui *et al.*;[13] however, our results also suggest that there is no semiconducting-metal transition at high pressures, contrary to the experimental evidence.

Density functional theory can reliably predict the structures of molecular crystals both at ambient and high pressure, and we are therefore confident in our results. However, our procedure in this work has been to determine high pressure structure by the application of hydrostatic pressure to the ambient experimental structure. It may be that the high pressure phase diagram of the $[Ni(ptdt)_2]$ crystal is complex, and that at the pressures considered in Refs. 13 and 14 there is a phase transition to a different crystal structure. As our calculations consist of zero Kelvin unit cell and structural relaxations, as opposed to more computationally expensive approaches such as *ab initio* molecular dynamics, we do not explore the P-T phase diagram, and it is thus possible that we would fail to detect such a transition. If this is the case, then it is conceivable that a different crystal structure could permit intermolecular packing such that the metallic state is stabilised. Unfortunately, there are no structural data that would allow us to explore this hypothesis.

IV. CONCLUSIONS

In this work we have explored in detail the structural and electronic properties of the $[Ni(ptdt)_2]$ crystal at ambient and high pressure. Our density functional calculations indicate that the $[Ni(ptdt)_2]$ molecule's structural integrity is maintained up to at least 22 GPa, and we are able to explain the observed trends in compression of the unit cell by invoking both the molecular and electronic structure. Structurally, we find no evidence of any distinct alterations in either molecular structure or intermolecular contacts that could account for an experimentally observed transition to metallic behaviour in the pressure range of 19–20.7 GPa. Our examination of the electronic structure indicates that this crystal is metallic, with a small density of states at the Fermi energy owing to the crossing band nature of the HOMO and LUMO; however, the resultant small Fermi surface may be invoked to explain both the large room-temperature conductivity of this crystal and the semiconducting-like temperature dependence of its resistivity.

The detailed form of the band structure is at odds with the description provided by tight-binding calculations, and indicates the importance of treating the different intermolecular interactions present. The resilience of the crossing-band nature of the HOMO and LUMO under the application of pressure explains why enhancement of a metallic state in this crystal is difficult, in agreement with experimental data. Our calculations indicate that there is no appreciable change in the electronic structure of this crystal over the range of 19.8–22 GPa, indicating that we find no evidence of a semiconductor-metal electronic transition. It is hypothesised that this discrepancy between our calculations and the experimental data could arise because of a high-pressure phase change of the $[Ni(ptdt)_2]$ crystal. A thorough investigation of this hypothesis requires the determination of the high pressure crystal structures, and it is our hope that this work will serve so as to stimulate structural studies of this crystal at high pressure.

Our results for the $[Ni(ptdt)_2]$ crystal suggest, in conjunction with recent work on the closely related $[Au(ptdt)_2]$

(Ref. 18) crystal, that the existence of metallicity in 2D layered single component materials may be more common than has been believed.

ACKNOWLEDGMENTS

The authors would like to thank HECToR, the UK supercomputing facility, and the University of Durham High Performance Computing Service for the provision of computing facilities used in this study. P.R.T. would like to acknowledge T. W. Hollins for the provision of data pertaining to the isolated molecule of [Ni(ptdt)$_2$].

[1]D. Jerome, Science **252**, 1509 (1991).
[2]J. Ferraris, V. Walatka, J. H. Perlstei, and D. O. Cowan, J. Am. Chem. Soc. **95**, 948 (1973).
[3]K. Kobayashi, E. Fujiwara, and H. Kobayashi, Chem. Rev. **104**, 5243 (2004).
[4]E. Ojima, B. Zh. Narymbetov, H. Fujiwara, H. Kobayashi, A. Kobayashi, K. Takimiya, T. Otsubo, and F. Ogura, Chem. Lett. **8**, 845 (1999).
[5]N. Thorup, G. Rindorf, H. Soling, and K. Bechgaard, Acta Crystallogr. **B37**, 1236 (1981).
[6]D. Jerome, M. Mazaud, M. Ribault, and K. Bechgaard, J. Phys. Lett. **41**, L95 (1980).
[7]H. J. Keller, *Chemistry and Physics of One-dimensional Metals*, NATO ASI Series B (Plenum, New York/London, 1977), Vol. 25.
[8]R. E. Peierls, *Quantum Theory of Solids* (Oxford University Press, Oxford, 1955), p. 108.
[9]C. Rovira, J. J. Novoa, J.-L. Mozos, P. Ordejon, and E. Candell, Phys. Rev. B **65**, 081104 (2002).
[10]H. Cui, Y. Okano, B. Zhou, A. Kobayashi, and H. Kobayashi, J. Am. Chem. Soc. **130**, 3738 (2008).
[11]K. Takemura, S. Minomura, O. Shimomura, and Y. Fujii, Phys. Rev. Lett. **45**, 1881 (1980).
[12]K. Shimizu, T. Yamauchi, N. Tamitani, N. Takeshita, M. Ishizuka, K. Amaya, and S. Endo, J. Supercond. **7**, 921 (1994).
[13]H. Cui, J. S. Brooks, A. Kobayashi, and H. Kobayashi, J. Am. Chem. Soc. **131**, 6358 (2009).
[14]H. Kobayashi, B. Zhou, A. Kobayashi, Y. Okano, E. Nishibori, M. Sakata, H. Cui, and J. Brooks, Physica B **405**, S303 (2010).
[15]A. Kobayashi, H. Tanaka, M. Kumasaki, H. Torii, B. Narymbetov, and T. Adachi, J. Am. Chem. Soc. **121**, 10763 (1999).
[16]A. Kobayashi, H. Tanaka, and H. Kobayashi, J. Mater. Chem. **11**, 2078 (2001).
[17]P. R. Tulip and S. P. Bates, J. Phys. Chem. C **113**, 19310 (2009).
[18]B. Zhou, H. Yajima, Y. Idobata, A. Kobayashi, T. Kobayashi, E. Nishibori, H. Sawa, and H. Kobayashi, Chem. Lett. **41**, 154 (2012).
[19]P. Hohenberg and W. Kohn, Phys. Rev. **136**(3B), B864 (1964).
[20]W. Kohn and L. J. Sham, Phys. Rev. **140**(4A), 133 (1965).
[21]S. J. Clark, M. D. Segall, C. J. Pickard *et al.*, Z. Kristallogr. **220**, 567 (2005).
[22]D. Vanderbilt, Phys. Rev. B **41**, 7892 (1990).
[23]H. J. Monkhorst and J. D. Pack, Phys. Rev. B **13**, 5188 (1976).
[24]J. P. Perdew and Y. Wang, Phys. Rev. B **46**, 12947 (1992).
[25]P. R. Tulip and S. J. Clark, Phys. Rev. B **71**, 195117 (2005).
[26]P. R. Tulip and S. P. Bates, Mol. Phys. **107**, 2201 (2009).
[27]R. O. Jones and O. Gunnarsson, Rev. Mod. Phys. **61**, 689 (1989).
[28]S. J. Clark and J. Robertson, Phys. Rev. B **82**, 085208 (2010).
[29]J. A. Chisholm, S. Motherwell, P. R. Tulip, S. Parsons, and S. J. Clark, Cryst. Growth Des. **5**, 1437 (2005).
[30]T. Mahmood, C. B. Cao, W. S. Khan, Z. Usman, F. K. Butt, and S. Hussain, Physica B Condens Matter **407**, 958 (2012).
[31]S. Lopez-Moren, P. Rodriguez-Hernandez, A. Munoz, A. H. Romero, and D. Errandonea, Phys. Rev. B **84**, 064108 (2011).
[32]H. Kimizuka, S. Ogata, J. Li, and Y. Shibutanin, Phys. Rev. B **75**, 054109 (2007).
[33]S. Ishibashi, K. Terakura, and A. Kobayashi, J. Phys. Soc. Jpn. **77**, 024702 (2008).